Send Orders for Reprints to reprints@benthamscience.net

200 *Current Nanoscience,* **2014,** *10,* **200-204**

Improvement of Elongation in Nanosurface Modified Bioglass/PLA Thin Film Composites

Innocent Jacob Macha[1,*], Besim Ben-Nissan[1] and Bruce Milthorpe[2]

[1]*School of Chemistry and Forensic Science, University of Technology Sydney, Australia;* [2]*Faculty of Science, University of Technology Sydney, Australia*

Abstract: One of the major challenges in the development of biomaterials is the adaptation of the complex elastic nature and elongation of human tissues during biomechanical functional loading. Composite materials present the most appropriate means of attempting to match the mechanical and biocompatibility requirements. Composite films from polylactic acid (PLA) and sol-gel derived bioglass (BG) powders with particle size ranging from 50-100 nm were produced by solution casting method. Three different bioglass mixtures of 0.1, 0.5 and 1% bioglass were prepared. Physico-chemical and morphological properties of bioglass, pure PLA and PLA composites were investigated using XRD, SEM and FTIR. Bioglass particles were further treated by nanolayer coating of 3-aminopropyltriethoxysilane (APTES) to improve its mechanical properties. The effects of surface treated bioglass on the fracture of the PLA/bioglass composites were investigated under tensile loading conditions. The results suggest by nano-surface treating the bioglass with 1% APTES significantly influences the percentage elongation of the PLA/bioglass composite at fracture. SEM shows more agglomeration of untreated bioglass within the composite. In the treated samples, a better distribution of nanosized bioglass within PLA matrix was observed. Nanolayer modified bioglass /PLA thin film composites may have a wide range of biomedical applications in tissue engineering with improved elastic properties.

Keywords: Bioglass, composites, elastic properties, nanolayer, polylactic acid, silane.

INTRODUCTION

Biomaterials, by definition, are "a non-drug substance suitable for inclusion in systems which augment or replace the function of bodily tissues or organs" [1]. Opportunities for organic/inorganic composites in the biomedical field arise from the numerous applications and the vastly different functional requirements. Biodegradable polymers and composites are very versatile for tissue engineering applications because they can be absorbed gradually by the human body without permanently retaining residuals in the implantation site [2]. Acid anhydrides, such as polylactic acid (PLA) and its co-polymers are among the group of biodegradable synthetic polymers that have been used in combination or alone for tissue engineering. PLA has been demonstrated to be biocompatible and to degrade into non-toxic components with a controllable degradation rate *in-vivo* [3-5].

Since their discovery by Hench and co-workers, bio-glasses and glass ceramics have attracted attention of many researchers [6]. Bioactive glass/biodegradable polymer composite materials have emerged in recent decades as new family of bioactive materials with applications ranging from structural implants to tissue engineering scaffolds [7]. Most of these composites that contain secondary particles show excessive agglomeration and non-homogeneous particle distribution within the matrix.

Effort has been devoted into functionalizing the surface of these secondary particles in order to improve adhesion, and their physico-chemical and mechanical properties. Surface modification of bioactive glasses to improve mechanical and biological properties of polylactic acid composites has been investigated using different grafting materials [8-11]. Past studies on improvement of mechanical properties have been focused on improving tensile strength, tensile modulus and impact energy of the bulk PLA composites [12].

*Address correspondence to this author at the School of Chemistry and Forensic Science, University of Technology, Sydney, PO BOX 123 BROADWAY 2007 NSW, Australia; Tel: +61450729436;
E-mail: innocent.macha@uts.edu.au

In this study, it was hypothesized that nanosurface treatment of bioglass particles may affect the chemical and physical properties of the surface layer and improve the mechanical properties of PLA/bioglass thin film composites.

MATERIALS AND METHODS

Materials

PLA was obtained from NatureWorks LLC, 3052D Australia. Materials for bioglass production, Tetraethyl orthosilicate (TEOS, $Si(OC_2H_9)_4$, 99.90%), Citric acid monohydrate (99%), Ethanol absolute (99.8%), Ammonium hydroxide solution (NH_4OH, 33%), Ammonium phosphate dibasic ($(NH_4)_2HPO_4$, 98%), Calcium nitrate tetrahydrate ($Ca(NO_3)_2.4H_2O$, 99.60%), PEG (Mw 20,000), acetic acid (99.7%) and (3-Aminopropyl)triethoxysilane (APTES) (99%) were obtained from Sigma Aldrich Australia.

METHODS

Sol-gel Bioglass

The procedures for preparing the bioglass powders (SiO_2:CaO:P_2O_5 (mol) 55:40:5) were based on the method reported in [13, 14] and further modified, and can be described as follows: 1) In an well-washed beaker equipped with a magnetic stirrer, 7.639 g calcium nitrate was dissolved in 120 mL of deionized water at room temperature. The TEOS-ethanol solution was created by diluting 9.167 g of TEOS in 60 mL of ethanol and added to the calcium nitrate solution. Then, citric acid was added into the solution to adjust the pH value to 1–2. The reaction mixture was kept stirring until a homogeneous and transparent solution was obtained. 2) Under vigorous stirring, the homogenous solution was slowly dropped into 1500 mL of ammoniated deionized water, in which 1.078 g of ammonium dibasic phosphate was dissolved in advance. During the dripping process, the pH value of solution was kept at around 11 using ammonia water. 3) After being stirred for 48 h and aged for 24 h, the precipitate was separated from the reaction solution by centrifugation at 3000 rpm, washed three times with deionized water, and finally separated in 200 mL of 2% PEG-water solution and kept still. 4) The precipitate was freeze dried for 24 hrs and fol-

1875-6786/14 $58.00+.00 © 2014 Bentham Science Publishers

lowed by calcination at 700 °C in a muffle furnace for 3 h, after which the white bioglass powders were obtained.

Bioglass Surface Functionalization

The deposition method from aqueous alcohol solutions was used to obtain silanated bioglass surfaces. A 95% ethanol-5% water solution was adjusted to pH 4.5-5.5 with acetic acid. Silane (3-aminopropyltriethoxysilane, APTES) was added with stirring to yield a 1% final concentration and then left for five minutes to allow fo hydrolysis and silanol formation. Bioglass powders were added suspended in the same solution and stirred for 2-3 minutes and then decanted the solution. The particles were rinsed twice briefly with ethanol and cured for 5-10 minutes at 110°C in an oven. The obtained silanised bioglass powders were stored in desiccator for further analyses.

Polymer Films and Composites

All the composites were prepared using a solvent casting technique described by [15] and modified by our team. PLA films were prepared by dissolving 0.50 g of polymer in 30ml of chloroform. The solution was transferred into 9 cm diameter petri dish for 24h, and chloroform was allowed to evaporate under low vacuum (in a desiccator). The films were stored in desiccators for further analyses. The same procedure with 15 minutes ultrasonication was employed to prepare PLA/Bioglass composites with loadings of 0.1, 0.5 and 1% bioglass.

Characterization

Calcination temperature was determined using simultaneous thermo-gravimetry and differential analysis (TG-DTA, SDT 2960, TA Instruments, New Castle, DE, USA) for the freeze dried bioglass. Sample weight of 30-40 mg was used during analysis under a circulating air environment with a heating rate of 10 °C/min from room temperature up to 1,100 °C.

The morphological analysis of bioglass, polymer films and composites samples was performed in Scanning Electron Microscopy (ZEISS Supra55VP, Zeiss, Sydney, Australia). Samples were fixed by mutual conductive adhesive tape on aluminium stubs and covered with carbon using a sputter coater. Images were taken at various magnifications at acceleration voltages of 5 kV to avoid beam damage to the polymer.

Phase analysis of the synthesized powders of Bioglass was conducted using primarily, X-ray diffraction using Seimens D5000 X-ray Diffractometer (Siemens, Bayswater, Australia) employing CuKα radiation (λ=0.15418 nm) with detector (X'celerator). The diffractometer was operated at 45 kV and 40 mA at a 2θ range of 20–70° employing a step size of 0.01 and a 4 s exposure.

The synthesized and surface functionalized bioglass were ground in an agate mortar and thoroughly mixed with KBr (FTIR Grade, 1% w/w). The FTIR spectra were collected using a Nicolet, Magna-IR 6700 Spectrometer FTIR (Thermo Fisher Scientific, Madison USA) in the range 4000–400 cm^{-1}. The mechanical characterization was performed by means of tensile and tear tests according to the ASTM D882 – 10 and ASTM D1004 – 13 standards respectively. Tests were carried out in a universal testing machine Instron 6022 equipped with a 5 kN load cell. Deformation was followed with windows based software.

RESULTS

Particle Size and Morphology of composites

Figs. (**1a** and **1b**) show the morphology of untreated bioglass PLA composites before tensile testing where the agglomerated bioglass particles were poorly distributed within the PLA matrix. Fig. (**1b**) shows the dispersion of nano size bioglass particles within polymer matrix at a higher magnification.

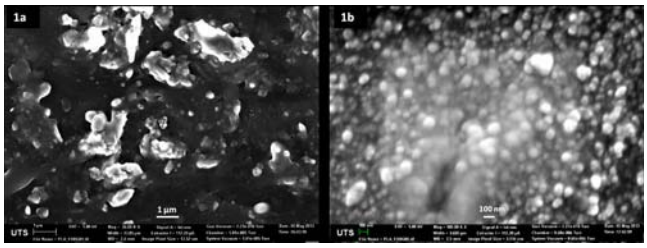


Fig. (1). SEM micrograph of PLA- untreated bioglass composite at different magnifications; **a**) 26KX and **b**) 100KX.

The distribution of the particles measured by Mastersizer 2000 (Malvern Instruments, Worcestershire, UK) indicated that particles or more accurately the agglomerates were between 1 to 100 micron in size. On the other hand SEM analysis of the treated bioglass composites showed both agglomerated and well dispersed powders with particles sizes ranging from 50-100 nm and some large agglomeration of particles were found within the matrix (Fig. **2a** and **2b**).

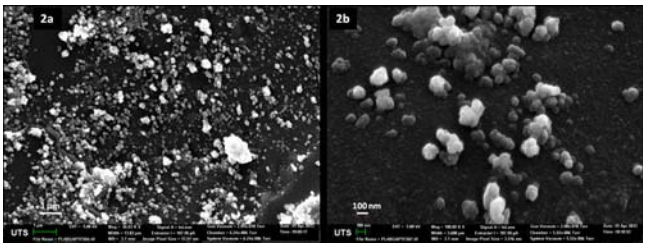


Fig. (2). SEM micrograph of PLA-1% APTES treated bioglass composite at different magnifications; **a**) 26KX and **b**) 100KX.

Sol-gel Bioglass

The Fourier Transform Infra Red (FTIR) spectrum of the calcined sol-gel bioglass is presented in Fig. (**3**). The FTIR spectra showed peaks at 1,050 and 463 cm^{-1}, corresponding to the Si-O-Si stretching and bending mode. The shoulder at about 796 cm^{-1} is attributed to the symmetric stretching of Si–O bond with nonbonding oxygen, namely, Si–NBO–Ca bending vibration mode. The peak at 557 cm^{-1} ascribed to the vibration modes of the P–O bond. However, it has to be considered that in this region both PO and SiO groups showed characteristic FT-IR peaks, resulting in a broad overlapping band [16]. The small shoulder at 2848 and peak at 1622 cm^{-1} are attributed to C-H stretching and O–H bending vibration band of PEG, which was used in the sol-gel bioglass synthesis. The peak at 3433 cm^{-1} attributed to O-H stretching of free water in the bioglass or in atmosphere. The amorphous nature of biglass was proved by not showing diffraction maxima in X ray diffraction (XRD) pattern.

Tensile and Failure Behaviour of the Composites

In Fig. (**4a**), the effect of APTES treated bioglass on elongation at break of PLA composites is presented. The prepared PLA composite with treated bioglass shows improved mechanical properties. The APTES treated material have a very high percentage elongation at break (an increase of 92 %) compared to pure PLA films and improvement of about 55% compared with untreated composites.

Fig. (**4b**) shows the tear resistance of PLA-untreated bioglass composites with 1, 3 and 5% bioglass loadings. It was observed that the tear resistant force and percentage elongation of PLA composites increases with an increase with the bioglass content from 1 to 3%. All data represent an average of four specimens.

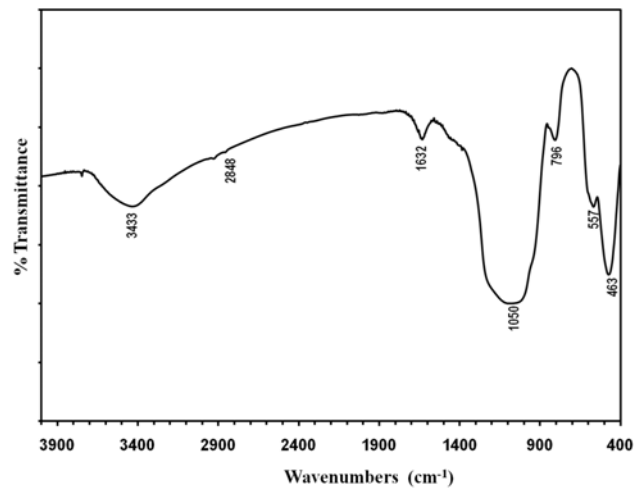


Fig. (3). FTIR spectra of calcined sol-gel bioglass.

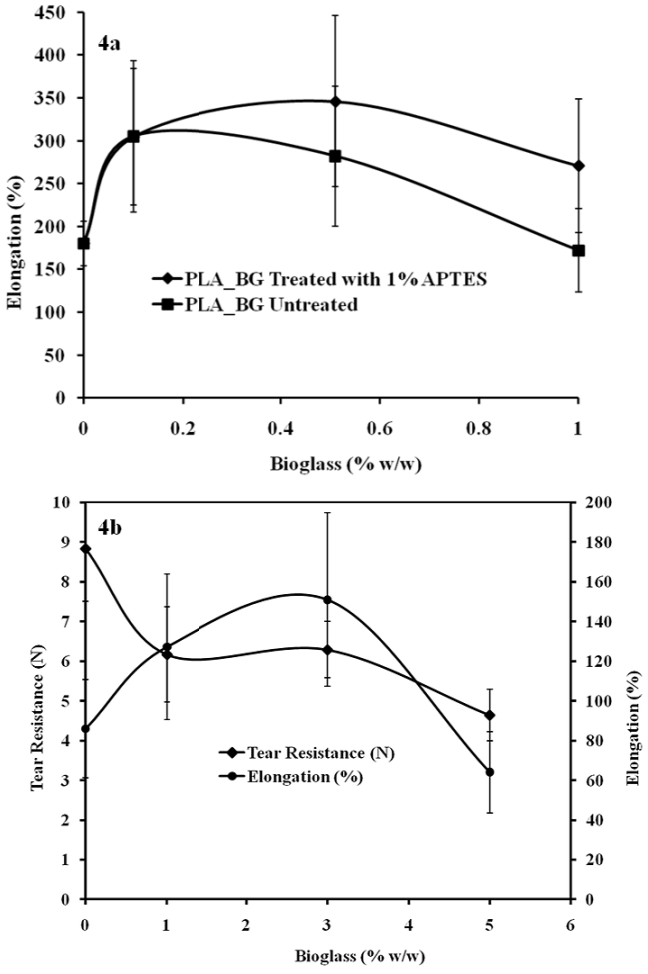


Fig. (4). a) Effect of treated and untreated bioglass on elongation at break of PLA composites under tensile testing **b**) Tear test showing tear resistance and percent elongation for untreated bioglass/PLA composites. Error bars represent standard deviation (SD).

The tensile results showed that pure PLA film has yield and failure strength of 140 MPa and 81 MPa respectively with elongation at failure of 180 %. The maximum elongation at break for untreated bioglass composites occurred at 0.1 % bioglass content with a yield and failure strength and elongation at break of 6.5 MPa, 4.8 MPa and 305%, respectively. On the other hand treated bioglass composites showed the maximum elongation at break of 346% with yield strength and failure strength of 5.2 MPa and 10.1 MPa respectively at 0.5% bioglass content.

Tear results for untreated bioglass composites showed that pure PLA film has a tear resistant load of 6.6 N while its tear failure resistance was 2.2 N with elongation at break of 86%. The maximum elongation at break occurred at 3% bioglass loading with tear yield resistance of 2.9 N, tear failure resistance of 2.1 N and elongation at break of 151%.

Fracture Morphology of Pure PLA and Composites

The morphology of pure PLA film after tensile testing is shown in Fig. (**5**). It was observed that the deformation behaviour is slightly different between the outer and inner surfaces of the films which may be due to a variations in the drying rates during fabrication. One of the fundamental features observed in PLA thin films after fracture is the "riverlines", which indicates clearly the crack growth direction. It is suggested that riverlines observed in multiple fractures initiated along the crack front during deformation and began to propagate on several slightly different planes and then subsequently converges onto one plane. Similar observations in other polymers also were reported [17]. Another feature observed on the fracture surface is the formation of "cusps", which appear on the fractured surface as raised platelets along riverlines [18].

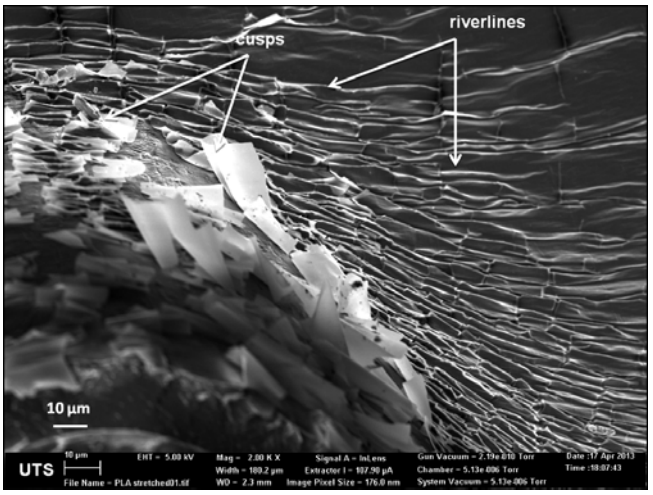


Fig. (5). SEM micrograph of tensile fractured pure PLA film showing the riverlines at the edge and the surface of the thin film.

In Fig. (**6**), the morphology of fractured PLA-untreated bioglass composite is shown. The bioglass particles in PLA matrix protruded cleanly from the matrix surface indicating a weak interfacial bonding and the compact agglomerated bioglass powders which are in some parts partially bonded to PLA matrix. The fracture seems to be initiated within the bioglass agglomerated particle and at the particle/PLA interface and spread outwards to the surface. In this particular juncture, agglomerated bioglass particle created voids within the matrix (Fig. **6**). These pores generate weak interfaces between the particles and the matrix. Furthermore, the particles are weakly adhered within the agglomerate itself due to weak adhesion of the individual particles and dissociate to smaller particles under load. The morphology of fracture is quite similar to pure PLA films with riverlines and cusps at the fracture point.

The presence of voids or pores within the polymer matrix could explain the difference in increased elongation of the PLA/bioglass composites compared to pure PLA films. The effect of voids on the elastic modulus of the composites could also be easily calculated theoretically and compared to the experimental results.

Pores act as stress concentrators in adjacent materials and give rise to anfractuous material networks that result in an uneven distribution of strains on loading [19].

Predictions of elastic properties of porous polymer composites using mixtures model developed by Alam [20] (Equation 1) are more accurate than classical mixture rules which do not incorporate sufficient details on how microstructural features such as pores affect the overall resistance to loading.

$$E_c = \left(E_r F_r \left(\frac{\overline{L_r}}{d_r}.\frac{1}{S_t}\right) + E_b F_{c,eff}\right).\frac{1}{\bar{A}}.\left(1 - \frac{w_{p,max}}{w}\right) \quad (1)$$

Where,

E - elastic modulus, $F_{c,\,eff}$ - effective area, F_r - particle fraction, $\overline{L_r}$ - mean reinforcement length, $\overline{D_r}$ - mean diameter, c - composites, b - binder (PLA), r - reinforcement (bioglass), S_t - stress transfer aspect ratio, W - sample width, $W_{p,\,max}$ - maximum pore length and $\overline{A}$ - mean anfractuosity.

Table **1** shows the comparison of elastic modulus estimation using both rules of mixtures given in equation 1, which incorporate pores effect and the experimentally measured values. As the results suggested, poor adhesion between bioglass and PLA introduces voids within the matrix which consequently affect the E_c of the composites.

Table 1. Summary of the Experimental and Calculated Elastic Modulus of Samples

Parameters	Calculated (Eq. 1) or published values	Experimental values	
		Treated	Untreated
Pure PLA Elongation %	180.0	NA	NA
Bioglass (0.1%) composite Elongation %	NA	304.5	305.1
Bioglass (0.5%) composite Elongation %	NA	345.9	282.1
Bioglass (1%) composite Elongation %	NA	270.9	171.9
E_r (GPa)	4.1[21]		
$E_{b,}$ (GPa)	35 [22]		
$E_{c\,(0.1\%\ Bioglass)}$ (GPa)±SD	3.8±0.2	3.2±1.0	2.8±1.0
$E_{c\,(0.5\%\ Bioglass)}$ (GPa) ±SD	3.6±0.1	3.1±1.2	3.2±1.2
$E_{c\,(1.0\ bioglass)}$ (GPa) ±SD	3.5±0.4	2.4±0.6	3.2±0.7

SD = Standard deviation

The morphological changes of fractured PLA-nanosurface treated bioglass with 1% APTES composites are shown in Figs. (**7a** and **7b**). As explained earlier, untreated bioglass particles agglomerated within the matrix with an average particle size of 1 to 100 μm. After surface treatment with 1% APTES, bioglass easily dispersed in all levels within matrix. In SEM observations particle size distribution of 5-50 nm was observed. A close examination of fractured surface of PLA-untreated bioglass and PLA-treated bioglass composite revealed a distinct difference in the fracture mode around the pores and at the bioglass-PLA matrix interface.

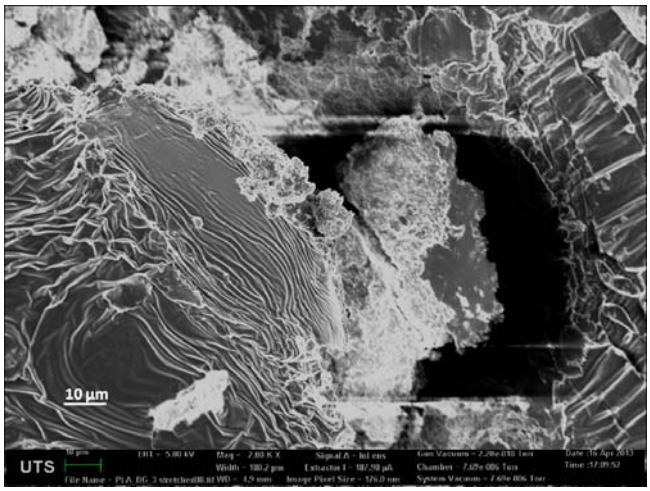


Fig. (6). SEM micrograph of fractured PLA-untreated bioglass composite showing agglomerated particles and related pore within PLA matrix (2KX).

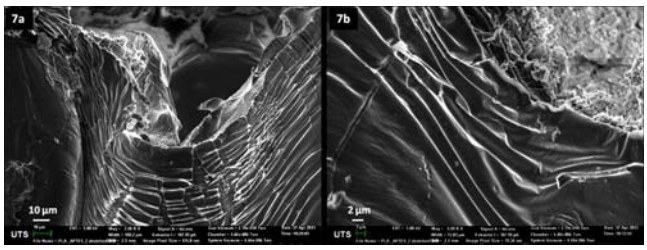


Fig. (7). SEM micrograph fractured treated bioglass PLA composite at different magnifications: **a**) 2 KX **b**) 5KX.

DISCUSSION

The fractured surface of treated bioglass PLA composites shows thinner riverlines around the particle-matrix interface indicating that the fracture did not start from the particle and spread outwards like in the untreated bioglass composites. It was observed that most of the bioglass agglomerated particles were protruded from the fracture surface indicating a weak interfacial adhesion. Higher magnification observations show the uniform distribution of bioglass particles within the matrix.

It can be suggested that surface treated bioglass with APTES provides better bonding between amine part of APTES and carbonyl group in PLA matrix that can contribute to a better interfacial adhesion than untreated ones especially at the nanoparticle level. In addition, it can be postulated that a better dispersion of treated bioglass in PLA matrix is observed due to the charge created on the outer part of the particle giving way to coulombic repulsion between the particles as shown in other functionalized nanoparticles [23].

Mechanical Properties of Pure PLA and Composites

Fig. (**4a**) shows the effect of APTES treated bioglass on the elongation at break of PLA-bioglass composites. SEM analysis of the treated bioglass composites (Figs. **2** and **7**) showed both agglomerated and well dispersed powders within polymer matrix. The improvement of elongation at break of PLA composites compared

with pure PLA films suggests that, the introduction of voids within PLA matrix due to poor interfacial adhesion between bioglass and PLA might be the cause of increase in composite flexibility. The effect of voids within PLA matrix on the elastic modulus was evaluated by comparing experimental values to values calculated using a mixtures' model for porous-polymer composites. The results do not show any significant differences between treated and untreated bioglass (55% difference) and the experimental elastic modulus correlate well with the calculated values.

In addition nanosurface treated bioglass with 1% APTES composites depicted higher elongation at break possibly due to coupling effect of APTES. APTES having bonded one side to bioglass surface, other sides are able to interpose between the linear chains of PLA and interfere with attractive hydrogen bonding and Van der Waals' forces between polymer chains, making it more flexible and hence enhancing interfacial adhesion between PLA and bioglass powders. Similar behaviour was observed in other composites using APTES [3]. All these microscopic features reinforce the reasoning why bioglass treated composites shown in Fig. (**7a** and **7b**) have improved flexibility with narrower riverlines at the fracture point.

Comparison of elongation at break in treated bioglass composite and pure PLA thin films showed an increase of 92%. In comparison to the untreated bioglass, an improvement of 55% was observed. It is envisaged that the improvement obtained could allow these materials to be used in wider tissue engineering applications where porosity and elongation are required.

In addition to tensile loading, tear tests were carried out according to the ASTM standards (ASTM D1004 - 13). Fig. (**4b**) shows the effect of bioglass contents on PLA bioglass composites elongation during tear test. It was observed that elongation at break during tear tests increases around 152% at 3% bioglass addition and then decreases afterwards. The different loading mode than tensile testing and poor interfacial adhesion during tears between bioglass and PLA matrix could explain the relatively lower elongation observed at break and at only higher bioglass contents than 3%.

CONCLUSIONS

PLA/ APTES nanosurface modified bioglass composites were prepared by solution casting method using different loadings of 0.1, 0.5 and 1% bioglass and showed improved elongation at break under tensile testing conditions. Bioglass treated with nanolayer of 1% APTES suggested to be effective in improving elongation at break of PLA/bioglass composites by enhancing dispersion and adhesion of bioglass particles in the polymer bioglass interfaces. Maximum elongation at break for PLA/untreated bioglass was 305% obtained at 0.1% bioglass which was an increase of 69.5% and decreased by -4.5% at 1% bioglass content compared with values for pure PLA films. For PLA/treated bioglass composites, the maximum elongation at break was 346% occurred at 0.5% bioglass loading with an increase of 92% then decreased to 50% at 1% bioglass compared to pure PLA film. PLA/treated bioglass composites shows an improvement on elongation at break of 55% at 1% bioglass compared to untreated bioglass composites. The morphology of the fracture surfaces showed that treated bioglass composites had stronger interfacial bonding at the PLA interface than untreated bioglass composites.

CONFLICT OF INTEREST

The authors confirm that this article content has no conflicts of interest.

Received: May 22, 2013 **Revised: June 25, 2013** **Accepted: July 8, 2013**

ACKNOWLEDGEMENTS

Declared none.

REFERENCES

[1] Ben-Nissan, B.; Pezzotti, G. Bioceramics. Processing Routes and Mechanical Evaluations. *J. Ceram. Soc. Jpn.*, **2002**, *110*, 601-608.

[2] Vroman, I.; Tighzert, L. Biodegradable Polymers. *Materials*, **2009**, *2*, 307-344.

[3] Chen, Q.; Liang, S; Thouas, G.A. Elastomeric biomaterials for tissue engineering. *Prog. Polym. Sci.*, **2013**, *38*, 584-671.

[4] Cai, X.; Tong, H.; Shen, X.; Chen, W.; Yan, J.; Hu, J. Preparation and characterization of homogeneous chitosan-polylactic acid/hydroxyapatite nanocomposite for bone tissue engineering and evaluation of its mechanical properties. *Acta Biomater.*, **2009**, *5*, 2693-2703.

[5] Guarino. V.; Causa, F.; Taddei, P.; di Foggia, M.; Ciapetti, G.; Martini, D.; Fagnano, C.; Baldini, N.; Ambrosio, L. Polylactic acid fibre-reinforced polycaprolactone scaffolds for bone tissue engineering. *Biomaterials*, **2008**, *29*, 3662-3670.

[6] Hench, L.L. Bioceramics: From Concept to Clinic. *J. Am. Ceram. Soc.*, **1991**, *74*, 1487-1510.

[7] Stamboulis, A.G.; Boccaccini, A.R.; Hench, L.L. Novel Biodegradable Polymer/Bioactive Glass Composites for Tissue Engineering Applications. *Adv. Eng. Mater.*, **2002**, *4*, 105-109.

[8] Verne, E.; Vitale-Brovarone, C.; Bui, E.; Bianchi, C.L.; Boccaccini, A.R. Surface functionalization of bioactive glasses. *J. Biomed. Mater. Res. A.*, **2009**, *90*, 981-992.

[9] Gao, Y.; Chang, J. Surface Modification of Bioactive Glasses and Preparation of PDLLA/Bioactive Glass Composite Films. *J. Biomater. Appl.*, **2009**, *24*, 119-138.

[10] Liu, A.X.; Hong, Z.K.; Zhuang, X.L.; Chen, X.S.; Cui, Y.; Liu, Y.; Jing, X. Surface modification of bioactive glass nanoparticles and the mechanical and biological properties of poly(L-lactide) composites. *Acta Biomater.*, **2008**, *4*, 1005-1015.

[11] Ling, L.; Wenwei, Y.; Yingjun, W.; Yinggang, Z.; Xiaofeng, C. Surface modification of bioactive glass and the preliminary study on the cell biocompatibility. *Acta Mater. Compos. Sin.*, **2011**, *1*, 114-118.

[12] Gerhardt, L-C.; Boccaccini, A.R. Bioactive Glass and Glass-Ceramic Scaffolds for Bone Tissue Engineering. *Materials*, **2010**, *3*, 3867-3910.

[13] Hench, L.L.; Greenspan, D. Interactions between Bioactive Glass and Collagen: A Review and New Perspectives. *J. Aust. Ceram. Soc.*, **2013**, *49*, 1-40.

[14] Hong, Z.; Reis, R.L.; Mano, J.F. Preparation and *in vitro* characterization of novel bioactive glass ceramic nanoparticles. *J. Biomed. Mater. Res. Part A.*, **2009**, *88*, 304-313.

[15] Buzarovska, A.;, Grozdanov, A. Biodegradable Poly(L-lactic acid)/TiO_2 Nanocomposites: Thermal Properties and Degradation. *J. Appl. Polym. Sci.*, **2012**, *123*, 2187-2193.

[16] Bianco, A.; Cacciotti, I.; Lombardi, M.; Montanaro, L. Si-substituted hydroxyapatite nanopowders: Synthesis, thermal stability and sinterability. *Mater. Res. Bull.*, **2009**, *44*, 345-354.

[17] Greenhalgh ES. *Failure analysis and fractographic of polymer composites*. Woodhead Publishing Limited: Cambridge, UK, **2009**.

[18] Lee, S. Mode II delamination failure mechanisms of polymer matrix composites. *J. Mater. Sci.*, **1997**, *32*, 1287-1295.

[19] Tsukrov, I.; Kachanov, M. Stress concentrations and microfracturing patterns in a brittle-elastic solid with interacting pores of diverse shapes. *Int. J. Solids Struct.*, **1997**, *34*, 2887-2904.

[20] Alam, P. A mixtures' model for porous particle–polymer composites. *Mech. Res. Commun.*, **2010**, *37*, 389-393.

[21] Garlotta, D. A Literature Review of Poly(Lactic Acid). *J. Polym. Environ.,* **2001**, *9*, 63-84.

[22] Thompson, I.D.; Hench, L.L. Mechanical properties of bioactive glasses, glass-ceramics and composites. *P. I. Mech Eng H.*, **1998**, *212*, 127-136.

[23] Thanh, N.T.K.; Green, L.A.W. Functionalisation of nanoparticles for biomedical applications. *Nano Today*, **2010**, *5*, 213-230.